

Statistical Measures and Selective Decay Principle for Generalized Euler Dynamics

G. Conti* and G. Badin†

Institute of Oceanography, Center for Earth System Research and Sustainability (CEN), University of Hamburg, Hamburg, Germany

(Dated: September 20, 2022)

We investigate the statistical mechanics of a family of two dimensional (2D) fluid flows, described by the generalized Euler equations, or α -models. These models describe both nonlocal and local dynamics, with one example of the latter one given by the Surface Quasi Geostrophy (SQG) model, for which the existence of singularities is still under debate. We aim to study the equilibrium mechanics, using initially a point-vortex approximation and then exploiting the full continuous equations, invoking the maximization of appropriate entropy functionals. The point-vortex approximation highlights an important difference between the 2D turbulence and local dynamics models. In the latter, it is in fact possible to derive a statistical measure only considering two conserved quantities as constraints for the maximization problem, the Hamiltonian and the angular impulse. This result does not hold for 2D turbulence. Both the continuous and the point vortex approximation allow for the derivation of mean field equations that act as constraints for the functional relation between the streamfunction and the active scalar of the model considered. Further, the analysis of the continuous equations suggests the existence of a selective decay principle for the whole family of models. To test these ideas we use numerical simulations of the partial differential equations of the α -models starting from different sets of initial conditions (i.c.s). For random i.c.s, all the solutions tend to a dipolar structure. The functional relation between the active scalar and the streamfunction shows an increase of nonlinearity with a decrease of the locality of the dynamics. We then test the evolution of the specific case of SQG for i.c.s in the form of a hyperbolic saddle, that is a candidate for the possible formation of singularity through a self-similar cascade though secondary instabilities. Results show the presence of a scale dependent selective decay associated to the breaking of the frontal structures emerging from the flow, suggesting a relation with the change of topology of the flow.

PACS numbers: 05.20.Jj; 05.65.+b; PACS 47.27.E-;PACS 92.10.Lq

Keywords: Turbulence; Surface Quasi-Geostrophic Dynamics; Vortex Dynamics; Selective Decay; Generalized Euler Equations

I. INTRODUCTION

Turbulence is a natural phenomenon that surrounds us, it is present around a waving hand as much as in geophysical and astrophysical objects. It is involved in the transport of passive tracers and drives the energy transfer between different scales. Although its importance, turbulence still remains one of the unsolved problems of physics. However, a statistical approach can be useful and profitable in the characterization of fluids undergoing turbulent motion [1–3].

In this study we investigate the equilibrium theory of a family of two dimensional incompressible fluid models that exhibits turbulence behavior using a statistical mechanics approach. These tools allow us to introduce a probability measure and a mean field equation that functionally relate the streamfunction and the active scalar, that is, they provide a constraint under which the solutions undergoing turbulent motion will have to tend. They also suggest how the solution can relax toward the

equilibrium. Although the derivations of the theories will follow straightforward from the well studied case of 2D turbulence, we think that it is worth to highlight some features that, at the best of our knowledge, have not been discussed in literature.

The governing equation for the family of models we study is

$$\frac{\partial q}{\partial t} + \mathcal{J}(\psi, q) = 0 \quad (1)$$

on the plane \mathcal{R}^2 , where $q(x, y, t)$ is an active scalar, or generalized potential vorticity, $\mathcal{J}(\psi, q) = \partial_x \psi \partial_y q - \partial_x q \partial_y \psi$ is the Jacobian determinant, and $\psi(x, y, t)$ is the streamfunction which satisfies the relationship

$$q = -(-\Delta)^{\alpha/2} \psi + \beta y = \zeta + \beta y, \quad (2)$$

with the parameter $\alpha \in \mathcal{R}$ that determines the degree of locality, or the range of interaction, of the model. In (2), ζ is the generalized relative vorticity and the term proportional to β is a dispersive term. These equations are known as generalized Euler equations or α -models (that must not be confused with Euler- α models [4, 5]). The effect of the α -parameter can be better understood setting $\beta = 0$ and transforming (2) in the Fourier space,

$$\hat{\psi}(\vec{k}) = -\left\| \vec{k} \right\|^{-\alpha} \hat{q}, \quad (3)$$

* Also at Foundation Euro-Mediterranean Center on Climate Change (CMCC), Bologna, Italy
giovanni.conti@uni-hamburg.de

† gualtiero.badin@uni-hamburg.de

where $\|\cdot\|$ is the usual L^2 norm, and \vec{k} is the 2D wavenumber vector. When α increases, fields become more decoupled. For $\alpha < 2$ the dynamics is said to be local, while for $\alpha > 2$ the dynamics is said to be non-local. These models were introduced by [6] have been studied for several values of α by e.g. [7–19]. When $\alpha = 2$, (1) and (2) describe the widely studied Euler equations with the active scalar representing the vorticity. In this case the dispersive term is related to the planetary gradient of the vorticity. The cases of $\alpha < 2$ and $\alpha > 2$ correspond to the so-called local and non-local dynamics. In this work we consider $\alpha \in (0, 3]$ since the cases with $\alpha > 3$ are unphysical, as they represent the case in which the effect of one vortex on another increases with distance.

Another case of physical interest is obtained for $\alpha = 1$, where (1) and (2) can be used to study the local dynamics of a stratified rapidly rotating flow upon a surface bounding a constant potential vorticity interior (e.g. the atmospheric tropopause or the oceanic surface). In this case the scalar field q takes the meaning of potential temperature or buoyancy. This model is called Surface Quasi Geostrophic (SQG) model [20–23]. It exhibits a characteristic forward energy cascade [24, 25], with consequent formation of small structures in the flow. This complementary behavior in respect to the one of 2D turbulence makes SQG a possible candidate for the forward cascade of temperature variance and the formation of frontal structures. For these reasons SQG is also a candidate for the explanation of the submesoscale dynamics (where the term submesoscale is here used in its oceanographic meaning, see e.g. [26]). As a consequence of this, SQG is considered also important for the mixing of passive tracers in the atmosphere and in the ocean [27–29]. For a study on the relationship between quasi geostrophic (QG) and SQG turbulence, see e.g. [30]. For the Hamiltonian and Nambu structure of SQG, see e.g. [23, 31]. From a mathematical point of view, SQG shows interesting analogies with the 3D Euler equation [32]. This analogy suggests that the study of the regularity of the SQG model could provide hints for the formation of singularities in the 3D Euler equation [6, 18, 32–56]. For SQG dynamics the dispersive term is related to the background potential temperature gradient [57].

We aim to study the equilibrium dynamics of this family of models first using a point-vortex approximation, and then considering a statistical theory valid for the continuous active scalar field. Statistical mechanics of 2D turbulence, based on a point-vortex approximation, started with Onsager [58] and the theory was further developed by e.g. [59–62]. In this approximation the vorticity field is substituted by a set of localized point vortices, which is the analogous of replacing a continuous mass distribution by a set of localized material points. The stability of SQG vortices has been studied by e.g. [63–69], while SQG point vortices have been studied by e.g. [18, 70, 71]. For the statistical dynamics of point vortices in 2D fluid dynamics see e.g. [58, 72–76].

The velocity statistic for point vortices of the gener-

alized Euler equation has been studied in [19]. In particular, [19] showed that while for $\alpha = 2$ the thermodynamic limit for the point vortex system does not exist due to logarithmic divergence with the number of vortices [72, 77, 78], this limit is instead defined for $\alpha \neq 2$.

We will treat the investigation of the equilibrium statistics for point vortices as an optimization problem invoking the maximum entropy principle. The idea is to maximize a functional, the entropy, under some constraint, given by the invariant of the theory, to find the shape of the probability distribution that governs the system. The extension of this machinery to the case $\alpha \neq 2$ raises interesting differences. In particular, if for 2D turbulence it is possible to define a measure and a mean field equation with the only use of the Hamiltonian function that describes the system, for $\alpha \neq 2$ we need necessarily to consider also another invariant quantity to regularize the measure, the angular impulse.

The second part of the work concerns with the study of the continuous system (1) using a modified form of the Miller-Robert-Sommeria (MRS) theory [79, 80] firstly introduced by [81] and further discussed by [82–84]. Continuous systems are particularly difficult to study as the set of stable states could be much larger than the set of the equilibrium states and other invariant measures than those predicted by the equilibrium theory could exist [16, 85]. Since in real situations some of the constraints can not be conserved due to the presence of forcing and/or dissipation, in the modified MRS theory some of the constraints and biases are taken into account by means of a prior distribution. This theory not only provides a way to define an equilibrium measure and a functional relation between the active scalar and the streamfunction, but it suggests and formalizes a selective decay principle for the entire family of α -models. That is, it provides a hint about the relaxation of the system toward the equilibrium.

Since the principle is suggested by a particular prior function, we investigate numerically the relaxation toward the equilibrium for different α -models, in a way that was previously explored by [16], but with the use of different initial conditions (i.c.s). Our work formalises part of the work reported by [16] and should be read as complementary to that.

In particular, in our work we study the evolution of different α -models starting from random i.c.s as well as from smooth analytical i.c.s corresponding to a hyperbolic saddle, which has been analysed in the literature as they are the candidate for the possible formation of singularities for the case $\alpha = 1$ [32].

For all the simulations we study the evolution of the ratio between generalized enstrophy and generalized energy, that for 2D turbulence has been used to set up in a rigorous way the selective decay principle [86].

The paper is organized as follows. In sec. II we build the statistical mechanics for the set of Hamiltonian equations of the point-vortex approximation for the generalized Euler equations, discussing the differences between

the 2D turbulence and the case $\alpha \neq 2$. In Section III we discuss a statistical theory for the continuous system and we show how this theory suggests a selective decay principle for the whole family of generalized models. In Section IV we investigate numerically the selective decay principle and the functional relation between the active scalar and the streamfunction. Finally in Section V we report the final discussions.

II. GENERALIZED POINT-VORTEX STATISTICAL THEORY FOR LOCAL DYNAMICS

Consider $\beta = 0$. In the point-vortex approximation we consider an active scalar concentrated in some points, so that it can be written in terms of the sum of Dirac delta functions, i.e a point-vortex located in the position $\vec{z}_0 = (x_0, y_0)$ generates an active scalar field of the form

$$q(\vec{z}) = \gamma \delta(\vec{z} - \vec{z}_0) \quad (4)$$

where γ is the generalized circulation. Even if q can represents an active scalar which might have a different meaning than vorticity, for example in the SQG case it represents the potential temperature, throughout the manuscript we will still call the entity arising from (4) as point-“vortex”. Solving (2) is possible to find the streamfunction and then, by means the usual derivation, the velocity field in the domain considered. The streamfunction is easily written in terms of the Green’s function of the problem considered

$$\psi(\vec{z}) = \int G_\alpha(\vec{z}, \vec{z}') q(\vec{z}') d\vec{z}', \quad (5)$$

where

$$G_2(\vec{z}, \vec{z}') = \frac{1}{2\pi} \ln(\|\vec{z} - \vec{z}'\|), \quad \alpha = 2, \quad (6a)$$

$$G_\alpha(\vec{z}, \vec{z}') = \phi(\alpha) \|\vec{z} - \vec{z}'\|^{\alpha-2}, \quad \alpha \neq 2, \quad (6b)$$

and

$$\phi(\alpha) = - \left\{ 2^\alpha \left[\Gamma\left(\frac{\alpha}{2}\right) \right]^2 \sin\left(\frac{\alpha\pi}{2}\right) \right\}^{-1}, \quad (7)$$

see for example [18, 87].

When $\alpha > 3$ the effect of one vortex on another increases with distance, and hence this case is considered unphysical [18]. Only the interval $\alpha \in (0, 3]$ will thus be considered.

A. Generalized Point-Vortex Equations

For the point-vortex approximation the resulting dynamics is Hamiltonian and is characterized by the conservation of energy, as well as the linear and angular momentum [88]. See e.g. [89–91] for reviews and [23, 92] for a discussion on symmetries and conservation laws.

Given N point vortices with circulations γ_i , $i = 1, \dots, N$, and with the coordinates of the vortices locations given by $\mathbf{z} = (x_1, y_1, \dots, x_N, y_N) = (\vec{z}_1, \dots, \vec{z}_N)$, the equations of motion for the vortices can be written as

$$\dot{\mathbf{z}} = \mathbf{D}_\alpha^{-1} \mathbf{J} \nabla_{\mathbf{z}} H_\alpha. \quad (8)$$

where $\mathbf{D}_\alpha = \text{diag}(\gamma_1, \gamma_1, \dots, \gamma_N, \gamma_N)$ when $\alpha = 2$ and $\mathbf{D}_\alpha = \text{diag}(\gamma_1/(2-\alpha), \gamma_1/(2-\alpha), \dots, \gamma_N/(2-\alpha), \gamma_N/(2-\alpha))$ when $\alpha \neq 2$, and \mathbf{J} is a block diagonal matrix with blocks given by symplectic matrices [23], and

$$H_2 = -\frac{1}{4\pi} \sum_{\substack{i,j=1 \\ j \neq i}}^N \gamma_i \gamma_j \log \|\vec{z}_i - \vec{z}_j\|, \quad (9a)$$

$$H_\alpha = -\frac{\phi(\alpha)}{2} \sum_{\substack{i,j=1 \\ j \neq i}}^N \frac{\gamma_i \gamma_j}{\|\vec{z}_i - \vec{z}_j\|^{2-\alpha}}, \quad \alpha \neq 2, \quad (9b)$$

is the Hamiltonian function, that is a conserved quantities representing the energy of the system.

Defining the canonical Poisson bracket, $[\cdot, \cdot]$, for the N -vortex problem as

$$[f, g] = \sum_{i=1}^N \frac{1}{\gamma_i} \left(\frac{\partial f}{\partial x_i} \frac{\partial g}{\partial y_i} - \frac{\partial g}{\partial x_i} \frac{\partial f}{\partial y_i} \right), \quad (10)$$

it is possible to show the conservation of the following quantities [18]

$$Q = \sum_{i=1}^N \gamma_i x_i, \quad (11a)$$

$$P = \sum_{i=1}^N \gamma_i y_i, \quad (11b)$$

$$I = \sum_{i=1}^N \gamma_i (x_i^2 + y_i^2) = \sum_{i=1}^N \gamma_i \|\vec{z}_i\|^2, \quad (11c)$$

that is, $[H_\alpha, Q] = [H_\alpha, P] = [H_\alpha, I] = 0$. The quantities Q , P and I are, respectively, the two components of the linear momentum and the angular impulse. Note that the only invariant depending on α is the Hamiltonian function. Note also that the conservation of these quantities might be dependent on the particular geometry considered, e.g. [93].

As will be more clear in the following sections, among all these entities, the Hamiltonian H_α and the angular impulse I should be regarded as particularly important. In fact, they will play a crucial role in determine the statistical measure for the point-vortex system with the α interaction. The linear momentum can be neglected in the definition of the measure because it appears as a

linear term that can be eliminated by a suitable change of coordinates.

Other conserved quantities are [18] the total circulation, the angular momentum and the conserved quantity $M = \sum_{i=1}^N \gamma_i I - (Q^2 + P^2)$. For the same reasons explained above, M does not introduce additional information to the definition of the measure and can thus be discarded. The same reasoning applies to the total circulation. The angular momentum for the point vortices is related to the Hamiltonian (9) and so it can be discarded too in the definition of the problem as will be set up in the next section.

B. Statistical Formulation

In order to investigate the equilibrium statistical mechanics of a large systems of Ordinary Differential Equations (ODEs), as the one described in (8), we need two important ingredients:

- the Liouville property, to ensure volume preserving or measure preserving feature in the phase space;
- conserved quantities that can be used as constraints in the maximization process of the Shannon entropy functional in order to obtain non-trivial results.

The following exposition will strictly resemble the one in [86], here generalized to the α -models of turbulence. Since the case of 2D turbulence has been extensively studied, see e.g. [61, 62], we will focus on $\alpha \neq 2$. Further, since the systems considered exhibits chaos due to their nonlinearity, we will assume ergodicity.

The Liouville property can be easily checked associating to (8) a flow map $\{\Phi^t(\mathbf{z})\}_{t \geq 0}$, $\Phi^t : \mathcal{R}^{2N} \mapsto \mathcal{R}^{2N}$ by

$$\frac{d}{dt} \Phi^t(\mathbf{z}) = \mathbf{F}(\Phi^t(\mathbf{z})), \quad \Phi^t(\mathbf{z})|_{t=0} = \mathbf{z}_0, \quad (12)$$

where

$$\mathbf{F}(\mathbf{z}) = \mathbf{D}_\alpha^{-1} \mathbf{J} \nabla_{\mathbf{z}} H_\alpha. \quad (13)$$

Since the vector field \mathbf{F} is divergence free, that is

$$\operatorname{div}_{\mathbf{z}} \mathbf{F}(\mathbf{z}) = 0, \quad (14)$$

the flow map (12) is volume preserving or measure preserving in the phase space [86, 94], and given an initial Probability Density Function (PDF) $p_0(\mathbf{z}, t = 0)$, then the PDF for any $t > 0$ can be defined by the pull-back of the initial probability density by means the flow map,

$$p(\mathbf{z}, t) = p_0((\Phi^t)^{-1}(\mathbf{z})), \quad (15)$$

that satisfies the Liouville equation

$$\frac{dp}{dt} + \mathbf{F} \cdot \nabla_{\mathbf{z}} p = 0. \quad (16)$$

So, $p(\mathbf{z}, t)$ is a PDF for all time.

The determination of the shape of $p(\mathbf{z}, t)$ can be studied invoking, as for the MRS theory, the maximization of the Shannon entropy functional defined as

$$\mathcal{S}(p) = - \int_{\mathcal{R}^{2N}} p(\mathbf{z}) \log p(\mathbf{z}) d\mathbf{z}, \quad (17)$$

where the Lebesgue measure is considered. Along with the Shannon entropy it is important not to forget the conserved quantities that act as constraints \mathcal{C} of the dynamics. So we need to find p^* such that

$$\mathcal{S}(p^*) = \max_{p \in \mathcal{C}} \mathcal{S}(p). \quad (18)$$

Note also that the entropy will be conserved at any time [86]. The research of the maximum can be done by means of the Lagrangian multipliers. In order to investigate the effects of locality in the probability density we need to consider the Hamiltonian constraint, being the only constraint depending of α . However, the resulting quantity of the optimization process is not integrable, due to divergences. Then, unless regularization, the use of the only Hamiltonian constraint is not allowed. The other important constraint that must be considered, together with the Hamiltonian, is the angular impulse (11c) that appears to be a natural regularizer. The other linear constraints can be neglected, because they can be eliminated with a proper change of variable.

In the following we also assume, without loss of generality, that $\gamma_k = 1$ for $1 \leq k \leq N$.

C. The H_α and I Constraints

Let us consider the energy (9) and the angular impulse (11c) as the only dynamical constraints for the probability. This means

$$\mathcal{C} = \mathcal{C}_0 \cap \mathcal{C}_\alpha \cap \mathcal{C}_I \quad (19)$$

where

$$\mathcal{C}_0 = \{p(\mathbf{z}) \mid p(\mathbf{z}) \geq 0 \wedge \int_{\mathcal{R}^{2N}} p(\mathbf{z}) d\mathbf{z} = 1\} \quad (20a)$$

$$\mathcal{C}_\alpha = \{p(\mathbf{z}) \mid \int_{\mathcal{R}^{2N}} H_\alpha(\mathbf{z}) p(\mathbf{z}) d\mathbf{z} = \bar{H}_\alpha\} \quad (20b)$$

$$\mathcal{C}_I = \{p(\mathbf{z}) \mid \int_{\mathcal{R}^{2N}} I(\mathbf{z}) p(\mathbf{z}) d\mathbf{z} = \bar{I}\}. \quad (20c)$$

The variational derivative of the entropy functional with respect the probability is

$$\frac{\delta \mathcal{S}}{\delta p} = -(1 + \log p), \quad (21)$$

while the variational derivative of the constraint \bar{C}_l is

$$\frac{\delta \bar{C}_l}{\delta p} = C_l(\mathbf{z}). \quad (22)$$

The Lagrangian multiplier method then yields

$$-(1 + \log p^*) = \lambda_0 + \lambda_\alpha C_\alpha(\mathbf{z}) + \lambda_I C_I(\mathbf{z}), \quad (23)$$

where λ_0 is the Lagrange multiplier related to the fact that p must be a probability density, and $\lambda_\alpha, \lambda_I$ are the Lagrange multipliers for the constraints related to the conserved quantities H_α and I . From (23) we can derive a measure that is analogous to the Gibbs measure in statistical mechanics

$$p^*(\mathbf{z}) = \mathcal{G}_{\lambda, N}(\mathbf{z}) = Z_N^{-1} \exp(-\lambda_\alpha H_\alpha(\mathbf{z}) - \lambda_I I(\mathbf{z})), \quad (24)$$

provided that it is normalizable, that is

$$Z_N = \int_{\mathcal{R}^{2N}} \exp(-\lambda_\alpha H_\alpha(\mathbf{z}) - \lambda_I I(\mathbf{z})) \, d\mathbf{z} < \infty. \quad (25)$$

Substituting the explicit form of H_α and I from (9) and (11c) into (25) yields

$$Z_N = \int_{\mathcal{R}^{2N}} \exp \left(\frac{\lambda_\alpha \phi(\alpha)}{2} \sum_{\substack{i,j=1 \\ j \neq i}}^N \frac{1}{\|\vec{z}_i - \vec{z}_j\|^{2-\alpha}} - \lambda_I \sum_{i=1}^N \|\vec{z}_i\|^2 \right) \, d\mathbf{z} \quad (26)$$

and in order to satisfy the integrability $\lambda_\alpha \phi(\alpha) < 0$, and $\lambda_I > 0$.

It is now clear that the use of the linear momentum in the constraints would result in linear terms in the measure that could be eliminated by using a suitable coordinates system.

Since we have a measure, we can define the average of a function $F(\mathbf{z})$ as

$$\langle F(\mathbf{z}) \rangle_{\mathcal{G}_{\lambda, N}} = \int_{\mathcal{R}^{2N}} F(\mathbf{z}) \mathcal{G}_{\lambda, N}(\mathbf{z}) \, d\mathbf{z}. \quad (27)$$

To properly fix the Lagrangian multipliers we need to satisfy the following integral equations

$$\langle H_\alpha \rangle_{\mathcal{G}_{\lambda, N}} = \int_{\mathcal{R}^{2N}} H_\alpha(\mathbf{z}) \mathcal{G}_{\lambda, N}(\mathbf{z}) \, d\mathbf{z} \quad (28a)$$

$$\langle I \rangle_{\mathcal{G}_{\lambda, N}} = \int_{\mathcal{R}^{2N}} I(\mathbf{z}) \mathcal{G}_{\lambda, N}(\mathbf{z}) \, d\mathbf{z}, \quad (28b)$$

that can be solved numerically.

Remark: As stated in the previous section, the Hamiltonian brings the dependence on α into the measure. However, without the use of the angular impulse the integral above would not converge if $\alpha < 2$.

The derivation of a mean field equation for the streamfunction for the general α -model is identical to the one for the case $\alpha = 2$ [61, 62, 86]. Replacing λ_α by λ_α/N ,

integrating (24) over $N-1$ variables to find the marginal distribution of a single vortex $p^*(\vec{z})$ with $\vec{z} \in \mathcal{R}^2$, and taking the thermodynamic limit $N \rightarrow \infty$ [19] we get the following *mean field equation*

$$-(-\Delta)^{\alpha/2} \psi^* = p^*(\vec{z}) = \frac{e^{-\lambda_\alpha \psi^*(\vec{z}) - \lambda_I \|\vec{z}\|^2}}{\int_{\mathcal{R}^2} e^{-\lambda_\alpha \psi^*(\vec{z}) - \lambda_I \|\vec{z}\|^2} \, d\vec{z}}. \quad (29)$$

Note that if we consider the following partition function

$$\mathcal{Z}_\alpha = \int_{\mathcal{R}^2} e^{-\lambda_\alpha \psi(\vec{z}) - \lambda_I \|\vec{z}\|^2} \, d\vec{z}, \quad (30)$$

the n -momentum of the streamfunction is derived as

$$\langle \psi(\vec{z})^n \rangle_{\mathcal{G}_\lambda} = \frac{(-1)^n}{\mathcal{Z}} \frac{\partial^n}{\partial \lambda_\alpha^n} \mathcal{Z}_\alpha, \quad (31)$$

and the mean field equation can be written as

$$-(-\Delta)^{\alpha/2} \psi = -\frac{1}{\lambda_\alpha} \frac{\delta}{\delta \psi} \log \mathcal{Z}_\alpha. \quad (32)$$

With a formally identical derivation as for $\alpha = 2$, it is possible to obtain a mean field equation for the generalized α -model of turbulence. However, if the angular impulse constraint could be neglected for $\alpha \geq 2$, that is for 2D turbulence and for non-local turbulence model, for the case of local turbulence $\alpha < 2$ is fundamental to reach the convergence of the probability measure. This is related to a fundamental change in the topology of the system hidden in the Green's function of the problem and then in the corresponding streamfunction.

Note that for different geometry, for example on a sphere, the ergodic hypothesis and the capability of the system of reaching a steady flow might be not valid, e.g. [93, 95].

III. CONTINUOUS CASE: EMPIRICAL STATISTICAL THEORY

The analytical results obtained in the previous section make use of the point-vortex approximation which is a strong simplification of the original problem. The finite size effects of the vortices can however modify the statistical measure found, moreover forcing and dissipation appearing at small scales make conservation of some constraints impossible. Further, there are physical situations in which external biases could influence the system and these biases can not be written in terms of constraints. Alternative statistical theories, based on a gran-canonical formulation of the MRS theory, have been proposed and discussed by e.g. [81–84]. In these theories the only constraints are the energy and circulation, while small scales effects are taken into account by means of a so called prior distribution.

Consider the continuous equations (1)-(2). We will look for a statistical distribution for the generalized potential vorticity ignoring the correlation from different

points, so we study the one point statistical information of the generalized potential vorticity. Following [86] we consider a probability density $\rho(\vec{z}, \nu)$ on $\Omega \times \mathcal{R}^1$, where Ω is the domain of our system, such that

$$\rho(\vec{z}, \nu) \geq 0, \quad \int_{\Omega} \int_{\mathcal{R}^1} \rho(\vec{z}, \nu) d\nu d\vec{z} = 1, \quad (33)$$

with

$$\int_{\Omega} f = \frac{1}{\Omega} \int_{\Omega} f. \quad (34)$$

We also require that for almost all $\vec{z} \in \Omega$, ρ is a probability density on \mathcal{R}^1 ,

$$\int_{\mathcal{R}^1} \rho(\vec{z}, \nu) d\nu = 1, \quad (35)$$

associated with the potential vorticity at the location \vec{z}

$$\int_{q_-}^{q_+} \rho(\vec{z}, \nu) d\nu = \text{Prob}\{q_- \leq q(\vec{z}) \leq q_+\}. \quad (36)$$

Along with these conditions we consider a prior distribution $\Pi_0(\vec{z}, \nu)$ also satisfying the condition (33) and (35). It is then necessary to modify the entropy functional to take into account the effect of the prior distribution. This can be easily done by mean of the relative entropy functional

$$\mathcal{S}(\rho, \Pi_0) \equiv - \int_{\Omega} \int_{\mathcal{R}^1} \rho(\vec{z}, \nu) \log \left(\frac{\rho(\vec{z}, \nu)}{\Pi_0(\vec{z}, \nu)} \right) d\nu d\vec{z}. \quad (37)$$

Proceeding as before we want to find the function ρ^* that maximizes (37) under certain constraints \mathcal{C}

$$\mathcal{S}(\rho^*, \Pi_0) = \max_{\rho \in \mathcal{C}} \mathcal{S}(\rho, \Pi_0). \quad (38)$$

In particular, we consider the normalization of the PDF, the mean generalized energy and the mean circulation represented using the one point statistic

$$\mathcal{C} = \mathcal{C}_0 \cap \mathcal{C}_E \cap \mathcal{C}_{\Gamma}, \quad (39)$$

where

$$\mathcal{C}_0 = \{\rho \mid M(\rho) = \int_{\mathcal{R}^1} \rho(\vec{z}, \nu) d\nu = 1, \quad \forall \vec{z} \in \Omega\}, \quad (40a)$$

$$\mathcal{C}_E = \{\rho \mid E(\rho) = - \int_{\Omega} \bar{\psi}(\bar{q} - \beta y) d\vec{z} = E_0\}, \quad (40b)$$

$$\mathcal{C}_{\Gamma} = \{\rho \mid \Gamma(\rho) = \int_{\Omega} \bar{q} d\vec{z} = \Gamma_0\}. \quad (40c)$$

The overbar represents the average with respect to the one point statistic, in particular

$$\bar{q}(\vec{z}) = \int_{\mathcal{R}^{\infty}} \nu \rho(\vec{z}, \nu) d\nu, \quad (41)$$

and then the correspondent streamfunction is

$$-(-\Delta)^{\alpha/2} \bar{\psi}(\vec{z}) + \beta y = \bar{q}(\vec{z}). \quad (42)$$

According to the Lagrange multiplier method we have

$$\rho^*(\vec{z}, \lambda) = \frac{\exp [\nu (\lambda_E \bar{\psi}^* - \lambda_{\Gamma})] \Pi_0(\vec{z}, \nu)}{\int_{\mathcal{R}^1} \exp [\nu (\lambda_E \bar{\psi}^* - \lambda_{\Gamma})] \Pi_0(\vec{z}, \nu) d\nu}, \quad (43)$$

where $\lambda_E, \lambda_{\Gamma}$ are the Lagrange multipliers of the problem, respectively related to the energy and circulation constraints. The mean field equation for q^* is then written as

$$\begin{aligned} \bar{q}^* &= -(-\Delta)^{\alpha/2} \bar{\psi}^*(\vec{z}) + \beta y \\ &= \frac{\int_{\mathcal{R}^1} \nu \exp [\nu (\lambda_E \bar{\psi}^* - \lambda_{\Gamma})] \Pi_0(\vec{z}, \nu)}{\int_{\mathcal{R}^1} \exp [\nu (\lambda_E \bar{\psi}^* - \lambda_{\Gamma})] \Pi_0(\vec{z}, \nu) d\nu}. \end{aligned} \quad (44)$$

Defining the partition function as

$$\mathcal{Z}(\psi, \vec{z}) = \int_{\mathcal{R}^1} \exp [\nu (\lambda_E \bar{\psi}^* - \lambda_{\Gamma})] \Pi_0(\vec{z}, \nu) d\nu, \quad (45)$$

the mean field equation (44) can be restated as

$$-(-\Delta)^{\alpha/2} \bar{\psi}^*(\vec{z}) + \beta y = \frac{1}{\lambda_E} \frac{\partial}{\partial \psi} \log \mathcal{Z}(\psi, \vec{z}) \Big|_{\psi=\bar{\psi}^*}. \quad (46)$$

In order to get more insight into the theory, we need to specify the form of the prior distribution, which will be done in the next Section.

A. Examples of Prior Distributions

1. The delta prior distribution and the point-vortex statistics

In order to compare the probability density and the mean field equation for the point-vortex statistics from the one point statistic, we need to modify a little bit the results of the previous section. If we use the normalization condition (33) and neglect the circulation constraint, the probability density (43) is transformed in

$$\rho^*(\vec{z}, \lambda) = \frac{\exp (\nu \lambda_E \bar{\psi}^*) \Pi_0(\vec{z}, \nu)}{\int_{\Omega} \int_{\mathcal{R}^1} \exp (\nu \lambda_E \bar{\psi}^*) \Pi_0(\vec{z}, \nu) d\nu d\vec{z}}. \quad (47)$$

The circulation can be taken into account considering that the most natural prior distribution for point vortices for N point vortices uniformly distributed with strength ω_0/N is [86]

$$\Pi_0(\nu) = \delta_{\omega_0}(\nu) \frac{d\vec{z}}{\Omega}. \quad (48)$$

Introducing (48) in (47) and setting $\beta = 0$ we obtain

$$\bar{q}^* = -(-\Delta)^{\alpha/2} \bar{\psi}^*(\vec{z}) = \frac{\omega_0 \Omega \exp (\omega_0 \lambda_E \bar{\psi}^*)}{\int \exp (\omega_0 \Omega \lambda_E \bar{\psi}^*) d\vec{z}}. \quad (49)$$

If $-\lambda_{\alpha} = \lambda_E \omega_0$, (49) reduces to (29) aside for the fact that the angular impulse has not been here considered as a constraint.

2. The Gaussian Prior Distribution and the Principle of Selective Decay

Deeper insight can be obtained modeling the small scales fluctuations of the generalized potential vorticity with Gaussian fluctuations with a given variance and zero mean. In fact, this kind of prior distribution generates a quadratic entropy functional [96] that naturally suggests the extension of the *selective decay principle* [86] to the entire family of the α -models of turbulence. Another consequence of this small scale parameterization is the linear relation arising between the generalized potential vorticity and the correspondent streamfunction.

Let us consider a prior distribution of the form

$$\Pi_0(\nu) = \sqrt{\frac{1}{2\pi\alpha^2}} \exp\left(-\frac{\nu^2}{2\alpha^2}\right). \quad (50)$$

The dependence on α is inspired by the fact that the range of interaction in the model under consideration affects also the distribution of the fluctuations. In particular, in (50) we place the standard deviation proportional to the range of interaction, that is α . The probability density (43) is thus reduced to

$$\rho^*(\vec{z}, \nu) = \sqrt{\frac{1}{2\pi\alpha^2}} \exp\left\{-\frac{[\nu + \alpha^2(\lambda_\Gamma - \lambda_E \bar{\psi}^*)]^2}{2\alpha^2}\right\}. \quad (51)$$

At each point of the domain we thus have

$$\int_{\mathcal{R}^1} \nu \rho^*(\vec{z}, \nu) d\nu = \alpha^2(\lambda_E \bar{\psi}^*(\vec{z}) - \lambda_\Gamma), \quad (52a)$$

$$\int_{\mathcal{R}^1} \nu^2 \rho^*(\vec{z}, \nu) d\nu = \alpha^2[1 + \alpha^2(\lambda_E \bar{\psi}^*(\vec{z}) - \lambda_\Gamma)^2]. \quad (52b)$$

Combining these results we obtain the following mean field equation

$$-(-\Delta)^{\alpha/2} \bar{\psi}^*(\vec{z}) + \beta y = \alpha^2(\lambda_E \bar{\psi}^*(\vec{z}) - \lambda_\Gamma). \quad (53)$$

This mean field equation is the fractional equivalent of the model introduced by [97] to study the inertial circulation in the ocean.

By means of (50) and (51), and neglecting the circulation constraint, the relative entropy functional can be written as

$$\mathcal{S}(\rho^*, \Pi_0) = -\frac{1}{\alpha^2} \mathcal{E}(\bar{q}^*), \quad (54)$$

where $\mathcal{E}(\bar{q}^*)$ represents the generalized potential enstrophy. Note that, aside for the explicit dependence on α on the r.h.s., both ρ^* and \bar{q}^* have an implicit dependence on α .

From (54), we can thus deduce that also for the α -models exists a *selective decay principle* which can be stated as follow: *After a long time, the solutions of the α -models of turbulence approach those states which minimize the generalized potential enstrophy for a given generalized energy.*

Note that in a turbulent field \mathcal{E} shows a scale dependence which depends on the wavenumber of the instabilities and on α (e.g. [6, 8]), suggesting the selective decay principle follows also a distinctive scale dependence which depends on the α model under consideration.

Setting β and λ_Γ to zero, the Lagrangian multiplier λ_E in (53) is determined by the eigenvalues of the fractional Laplacian. Alternatively, since the streamfunction is determined up to a constant, λ_Γ can be reabsorbed into ψ^* without loss of generality. For a double periodic domain of length $L = 2\pi$, the smallest eigenvalue is $\mu = \alpha^2 \lambda_E = 1$ and the streamfunction reduces to

$$\psi(x, y) = a \sin(x) + b \sin(y) + c \cos(x) + d \cos(y), \quad (55)$$

as for the $\alpha = 2$ case [86]. In the case of $a = A$, $b = c = d = 0$ the solution corresponds to a simple shear flow, while when $a = b = A$, $c = d = 0$ the solution corresponds to an array of 2D swirling vortices. In section IV A we will find that this is the case to which our system evolves when we employ random Gaussian initial conditions.

Remark: *Different prior distributions lead to different mean field equations, which can be also nonlinear [96, 98, 99]. Although the Gaussian prior distribution generates a quadratic entropy functional, suggesting thus the extension of selective decay principle also for all the α -models, nonlinear mean field equations can be particularly important in geophysical flow [100, 101]. Moreover, a nonlinear prior distribution can give rise to a higher degree polynomial entropy functional, that can thus be used to explain flow transitions [96, 102].*

IV. NUMERICAL INVESTIGATIONS

In the previous section, the existence of a selective decay principle was suggested by a probability density obtained with a particular prior distribution. At this point, nothing grants that this principle hold in general. In the following, we will explore numerically the evolution of different turbulent flows for different values of α in order to prove the existence and the consequences of the selective decay principle.

We perform numerical simulations using a semi-spectral scheme in a double periodic domain of length $L = 2\pi$. The Jacobian is computed by means of the Arakawa [103] discretization. Time integration is performed with a fourth order explicit Runge-Kutta scheme. To avoid the accumulation of enstrophy at small scales, we multiply each Fourier mode by an exponential function of the form $f(w) = \exp(-aw^m)$ where w is a variable proportional to the meridional or zonal wavenumbers [53, 104, 105]. We use two sets of initial conditions, for each set we perform the simulations for different α . The β dispersion will not be considered so that $q = \zeta$.

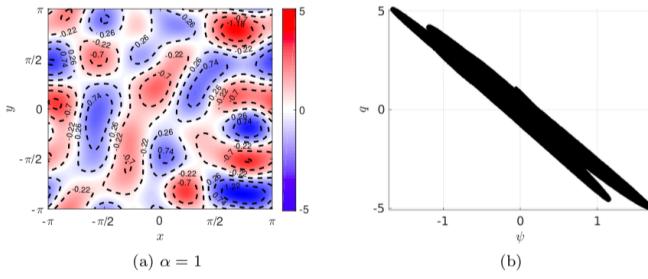


FIG. 1. Random initial condition for SQG ($\alpha = 1$). The left panel shows the q field (colours) with the superimposed streamfunction (dashed line). The right panel shows the corresponding $\psi - q$ relation.

A. Random Initial Conditions

For this set of simulations we consider a random $q(\vec{z}, 0)$ field with horizontal grid resolution to 512×512 points, obtained by the inversion of the streamfunction

$$\hat{\psi}(\vec{k}, 0) \propto \exp[-(\|\vec{k}\| - k_0)^2] \quad (56)$$

with $k_0 = 3$. The streamfunction is normalized so that $1/2 \|\vec{k}\|^2 \hat{\psi}(\vec{k}, 0)^2 = E_0$, with $E_0 = 4 \times 10^3$. When $\alpha = 1$, E_0 represents the surface kinetic energy. We assume a small Newtonian viscosity with dissipation coefficient $\mu = 10^{-3}$ as in [86]. The coefficient for the exponential filter in the Fourier space are set to $a = 36$, $m = 16$. All the simulations are run until $T = 10^3$ with time step $\Delta t = 5 \times 10^{-3}$. The experiments are performed for the different values of $\alpha = 0.5, 1, 2, 3$.

Note that the initial streamfunction is equal for all the different models, but the correspondent q field will change accordingly to (3). The left panel of Figure 1 shows the active scalar and the correspondent streamfunction (dashed line) for the SQG case. The right panel shows the $\psi - q$ relation for the same fields.

Starting from these initial conditions all the α -models relax toward a dipole solution (Figure 2). The $\psi - q$ relation for different α show that for short range interaction ($\alpha = 0.5$) the functional relation is approximately linear, with nonlinearity increasing with increasing α . Notice that since the initial condition posses non-null zonal and meridional averages, the dipole structure translates in the periodic domain without changing its structure. For this reason, the results shown in Figure 2 refer only to the last step of the time integration rather than to a time average of the fields.

Figure 3 shows the behaviour in time of the ratio between the generalized enstrophy and energy, $R = \mathcal{E}/E$, which has been used to express in a mathematical rigorous way the selective decay principle for $\alpha = 2$ [16, 86]. It should be noted that for $\alpha = 2$, the quantity $P = (2\pi/L)^\alpha E/\mathcal{E}$, that for our simulations reduce to

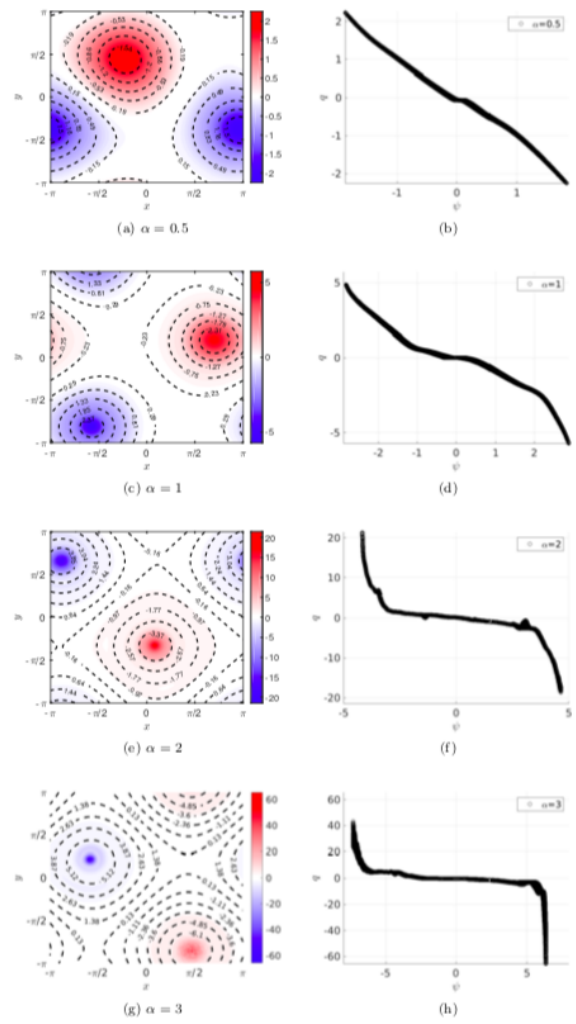


FIG. 2. Evolution of the scalar field and the streamfunctions at $T = 10^3$ for different models, $\alpha = 0.5, 1, 2, 3$. In the left column is plotted the q field with the superimposed streamfunction (dashed line). In the right column is reported the functional relation $\psi - q$ for the corresponding values of α .

$P = R^{-1}$, has been observed to be $P \approx 1$ when a general unstable conditions relaxes toward an equilibrium state [106].

Figure 3 shows that R exhibits a decay for all the α models. The decay of R is faster for increasing values α , with the slope of R getting steeper for models with a more non-local behaviour, i.e. with longer range of interaction. This can be explained considering that models with longer range of interaction are able to “transmit information” better between distant points of the domain and can thus adjust more efficiently. The different decay between the α -models can be also seen in terms of depletion of nonlinearity [54, 107]: in the presence of non-local interactions, the depletion of nonlinearity is faster than for systems with local interactions, which need thus more time for equilibration to happen. Integrations with lower

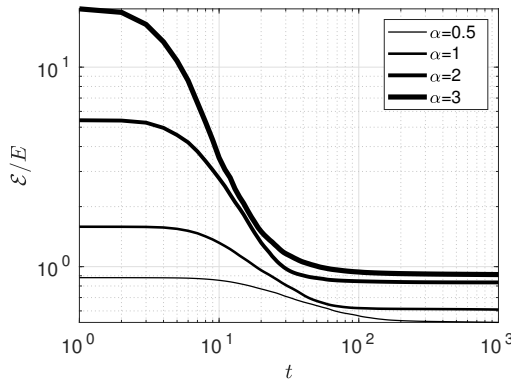


FIG. 3. Evolution of $R = \mathcal{E}/E$ for different α -models starting from random i.c.s.

values of α reach the steady state with more difficulty. This can be seen e.g. in Figure 2, where the vortices of the dipole for the cases $\alpha = 0.5, 1$ are not as symmetric as the ones produced for the cases with $\alpha = 2, 3$.

The results here found differ from the results found by [16]. In their study, [16] used as i.c.s a bimodal distribution centred at low wavenumbers. Their results show the formation of large unidirectional structures or monopoles for lower values of α , with a continuous transition to a dipole for higher values of the same parameter. [16] found also that increasing α , the $\psi - q$ relation shows a transition between a sinh-like to a tanh-like functional. The differences between the results found here and the ones found by [16] suggest that the selective decay acts toward the formation of structures that may differ greatly due to the different choices of the prior distribution.

B. Hyperbolic Saddle

As a second set of i.c.s, we explore the selective decay associated to a hyperbolic saddle geometry, which has aroused a certain interest since early studies have suggested that it could be able to develop singularities for the inviscid $\alpha = 1$ (SQG) case [32, 33, 37, 53]. The possible existence of singularities in SQG is suggested by considering the horizontal gradient of (1), which yields

$$\frac{D\nabla q}{Dt} = \nabla q \cdot \nabla \vec{u}, \quad (57)$$

where D/Dt represents the material derivative. The resulting equation is a 2D counterpart of the 3D Euler equation, with $\nabla q \leftrightarrow \vec{\omega}_{3D}$ and with an emerging 2D stretching term on the r.h.s which might be responsible for the blow-up. Notice that for $\alpha = 2$, the r.h.s. of (57) is zero and no blow-up occurs. The finite time blow-up criteria of the resulting equation is the correspondent of a Beale-Kato-Majda criteria [108], which in the case of

SQG reads as [32]

$$\int_0^T \|\nabla q\|_{L^\infty}(s) ds \rightarrow \infty \text{ as } T \rightarrow T^*. \quad (58)$$

Successive studies have ruled out the formation of singularities in the specific case of the hyperbolic saddle geometry [36], with $\nabla q \propto \exp \exp t$. Other studies [6, 52, 55, 56] have however suggested that during its time evolution, the hyperbolic saddle forms a filament which undergoes secondary instabilities and that these instabilities can lead to a finite time singularity via a self-similar cascade of ∇q toward smaller and smaller scales.

In the following we will compare the evolution of the hyperbolic saddle geometry for the cases $\alpha = 1$ and $\alpha = 2$. The initial condition is given by

$$q(\vec{z}) = \sin(x) \sin(y) + \cos(y), \quad (59)$$

for both $\alpha = 1$ and $\alpha = 2$. Simulations are performed with increasing grid resolutions 512×512 , 1024×1024 , 2048×2048 and 4096×4096 .

We simulate the flow until $T = 16$. For the low resolution case of 512×512 , we simulate the flow until $T = 5 \times 10^3$. All simulations are performed with time step $\Delta t = 10^{-3}$.

Selective decay requires the presence of dissipation, which in our case is given only by the exponential filter as the dissipation coefficient is set as $\mu = 0$. The parameters for the filter in the Fourier space are set as in [53], that is $a = 36$, $m = 19$.

Figure 4 shows the initial active scalar field with the correspondent streamfunction (dashed line) in the left panel for $\alpha = 1$ and, the functional relation $\psi - q$ on the right.

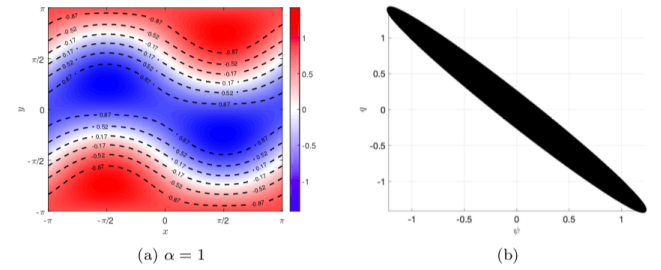


FIG. 4. As in Figure 1, but for the initial conditions (59). The grid resolution here is 4096×4096 grid points.

Figure 5 shows the evolution of the flow, which consists in an intensification of the front at $T = 8$, a breaking down of the front by means of secondary instabilities at $T = 11.5$ and a disruption of the central filament at $T = 15.9$.

The scatter plots of q versus ψ on the right panels of figure 5 highlight the nonlinear relations out of the equilibrium between the active scalar and the streamfunction during the three stages of the development of the flow.

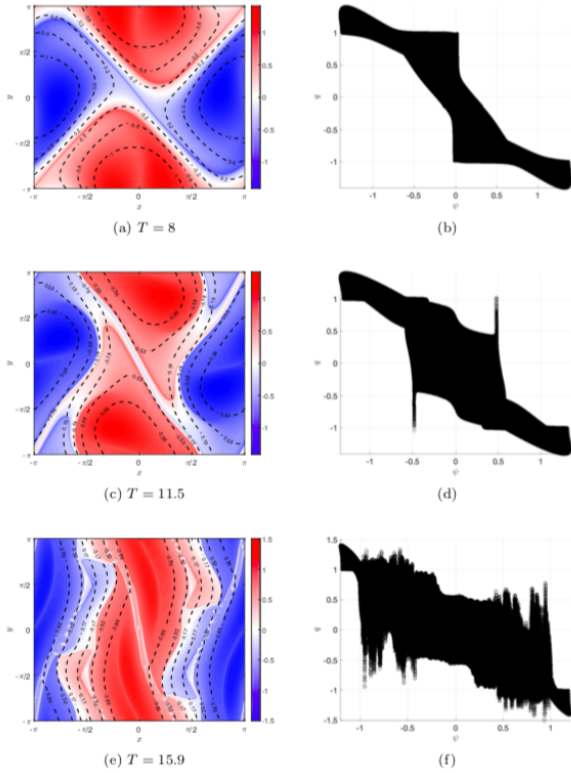


FIG. 5. Left panels: q (coloured) and ψ (dashed lines) fields for the case $\alpha = 1$ (a) during the front intensification at $T = 8$, (c) during the front deformation at $T = 11.5$ and (e) after the disruption of the front at $T = 15.9$. Right panels: scatter plots of q versus ψ for the corresponding three times. The grid resolution is 4096×4096 .

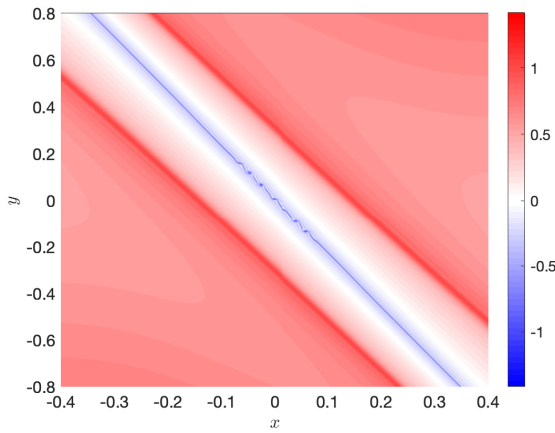


FIG. 6. Central region of Fig. 5c at $T = 11.5$, showing the deformation of the front by means of secondary instabilities.

The form of the secondary instabilities which are responsible for the breaking of the central filament is shown in Figure 6. As noted by [52], even if the simulations are

able to resolve the secondary filament connecting these secondary instabilities, even for the highest resolution simulation the formation of these happens when the evolution of the flow is past its inviscid stage. The study of the breaking of the central filament at different resolutions will however give us hints about the possibility to study this phenomena making use of the selective dissipation.

The trend of the ratio R (Figure 7) shows that even at the end of the integrations the simulations are not able to reach an equilibrium. At $T = 5 \times 10^3$ the solutions still exhibit oscillations and the ratio R is not completely equilibrated.

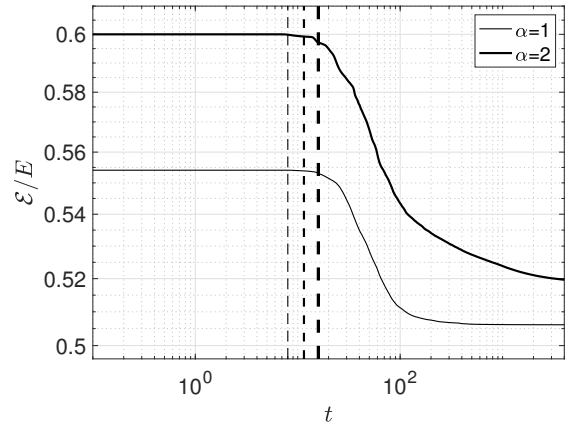


FIG. 7. The R ratio for the simulations with initial condition (59). The vertical dashed lines represent the times $T = 8$, $T = 11.5$ and $T = 15.9$ respectively.

Thus to study the reaching of a final quasi steady state, we consider a time average of the fields on the last ~ 80 eddy turnover times, here defined as $T_{eddy} = (2\pi)^{2-\alpha}/q_{rms}$ (Figure 8). For both $\alpha = 1, 2$, the flow evolves toward a meridional structure. The comparison between the two cases shows also that, in agreement with the results found for the case of random i.c.s, for $\alpha = 1$ the functional relation $\psi - q$ is approximately linear, while for $\alpha = 2$ the nonlinearity is intensified.

For $\alpha = 1$ and at 4096×4096 resolution, R begins to strongly decay at the moment of the breaking of the central filament by the action of the secondary instabilities at $T \sim 11.5$ figure 9. It is interesting to compare the trends in time of R and of the quantity $\max\|\nabla\theta\|$, which enters the modified Beale-Kato-Majda criteria (58). Figure 10 shows that at $T \sim 11.5$ this quantity starts to exhibit non-smooth oscillations associated with the breaking of the filament by secondary instabilities.

These results show that *the selective decay appears when the flow becomes unstable by secondary instabilities and these instabilities change its topology, allowing for the flow to evolve to a state with minimum values of R .*

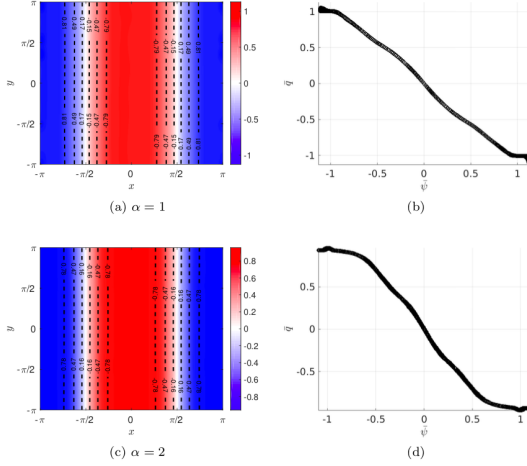


FIG. 8. Left panels: time average of the q and ψ fields over the last ~ 80 eddy turnover times. Right panels: functional relation between the same two fields for the case (a,b) $\alpha = 1$, and (c,d) $\alpha = 2$. For this long run the grid resolution used is set to 512×512 grid points.

The comparison of the results at 4096×4096 resolution with the integrations at lower resolution is in agreement with the observation that selective decay is scale-dependent. Lowering the resolution shows an anticipation of the selective decay, in agreement with the anticipated breaking of the central filament at lower resolution.

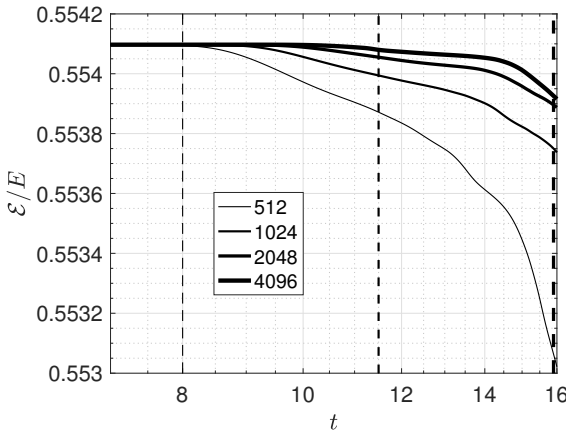


FIG. 9. Decay of R for $\alpha = 1$ and different resolutions. The vertical dashed lines represent the times $T = 8$, $T = 11.5$ and $T = 15.9$ respectively.

V. CONCLUSIONS

In this work we have investigated a family of turbulent models described by the generalized Euler equations

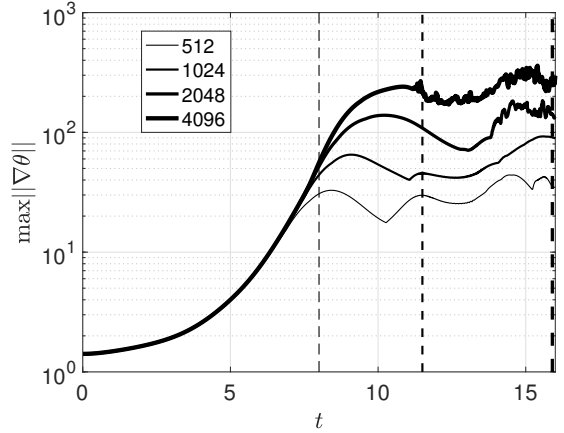


FIG. 10. Behavior of $\max\|\nabla\theta\|$ for different resolutions. The vertical dashed lines represent the times $T = 8$, $T = 11.5$ and $T = 15.9$ respectively.

studying their long time statistical equilibrium. Similarly to the MRS theory [79, 80] we invoked the maximization of appropriate entropy functionals translating the research of the probability measure in an optimization problem with constraints given by opportunely chosen conserved quantities of the system. This allowed the definition of some relations, the mean field equations, that play the role of constraints for some possible final state for the turbulent flow. It is important to stress that the set of stable states could be much larger than that the one arising by the equilibrium statistical theories, implying thus the possible existence of other invariant measures. Other problems in the application of the MRS theory arise also in regard to the ergodic hypothesis and the conservation of some of the quantities used as constraints for other geometries [93, 95]. Nevertheless, the use of statistical mechanics suggests deep differences between the considered models but also common principles that describe how the flow have to relax toward the equilibrium solutions.

The point-vortex approximation shows that the probability measure exhibits substantial differences between the case of 2D turbulence, $\alpha = 2$, and the case of local dynamics, i.e. $\alpha < 2$. In the latter case, the probability measure can be defined by exploitation of only a second constraint, the angular impulse, other than the Hamiltonian function which is sufficient for the 2D turbulence.

The continuous case shows that, while all models evolve toward a final dipolar structure, increasing values of α correspond to a stronger nonlinearity in the $\psi - q$ relation and a faster transition toward the final state. Importantly, the differences between our results and the results from previous studies [16] suggest that the selective decay acts toward the formation of structures that may differ greatly due to the different choices of the prior distribution.

Finally, we have investigated the role of the selective

decay in the transition to the final state for i.c.s given by a hyperbolic saddle for the case of $\alpha = 1$, which is a possible candidate for the emergence of singularities in SQG. In this case, the violent decay of the ratio between the generalized enstrophy and energy corresponds to the rise of secondary instabilities and the subsequent breaking of the central filament of the flow, suggesting thus a relationship between the selective decay and the change

of topology of the flow.

ACKNOWLEDGMENTS

This work was partially funded by the research grant DFG BA5068/9-1.

[1] R.H. Kraichnan, *Phys. Fluids* **10**(7), 1417 (1967)

[2] R.H. Kraichnan, *J. Fluid Mech.* **67**(1), 155 (1975)

[3] U. Frisch, *Turbulence: The Legacy of A. N. Kolmogorov* (Cambridge University Press, 1995)

[4] D.D. Holm, J.E. Marsden, T.S. Ratiu, *Adv. Math.* **137**(1), 1 (1998)

[5] G. Badin, M. Oliver, S. Vasylkevych, *J. Phys. A: Math. Theor.* **51**(45), 455501 (2018)

[6] R. Pierrehumbert, I. Held, K. Swanson, *Chaos Solit. Fract.* **4**, 1111 (1994)

[7] S. Weinstein, P. Olson, D. Yuen, *Geophys. Astro. Fluid Dyn.* **47**(1-4), 157 (1989)

[8] K.S. Smith, G. Boccaletti, C. Henning, I. Marinov, C. Tam, I. Held, G.K. Vallis, *J. Fluid Mech.* **469**, 13 (2002)

[9] C. Tran, T. Shepherd, *Physica D* **165**(3), 199 (2002)

[10] C. Tran, *Physica D* **191**(1), 137 (2004)

[11] D. Bernard, G. Boffetta, A. Celani, G. Falkovich, *Phys. Rev. Lett.* **98**(2), 024501 (2007)

[12] C. Tran, D. Dritschel, R. Scott, *Phys. Rev. E* **81**(1), 016301 (2010)

[13] B. Burgess, T. Shepherd, *J. Fluid Mech.* **725**, 332 (2013)

[14] B. Burgess, R. Scott, T. Shepherd, *J. Fluid Mech.* **767**, 467 (2015)

[15] N. Schorghofer, *Phys. Rev. E* **61**, 6568 (2000)

[16] A. Venaille, T. Dauxois, S. Ruffo, *Phys. Rev. E* **92**, 011001 (2015)

[17] A. Foussard, S. Berti, X. Perrot, G. Lapeyre, *J. Fluid Mech.* **821**, 358 (2017)

[18] G. Badin, A.M. Barry, *Phys. Rev. E* **98**, 023110 (2018)

[19] G. Conti, G. Badin, *Geophys. Astro. Fluid Dyn.* (2019). Doi:10.1080/03091929.2019.1572750

[20] W. Blumen, *J. Atmos. Sci.* **35**, 774 (1978)

[21] I.M. Held, R.T. Pierrehumbert, S.T. Garner, K.L. Swanson, *J. Fluid Mech.* **282**, 1 (1995)

[22] G. Lapeyre, *Fluids* **2**, 7 (2017)

[23] G. Badin, F. Crisciani, *Variational Formulation of Fluid and Geophysical Fluid Dynamics: Mechanics, Symmetries and Conservation Laws* (Springer, 2018)

[24] R. Tulloch, K. Smith, *Proc. Natl. Acad. Sci. U.S.A.* **103**(40), 14690 (2006)

[25] X. Capet, P. Klein, B. Hua, G. Lapeyre, J. McWilliams, *J. Fluid Mech.* **604**, 165 (2008)

[26] J.C. McWilliams, *Proc. Roy. Soc. A* **472**(2189), 20160117 (2016)

[27] G. Badin, A. Tandon, A. Mahadevan, *J. Phys. Oceanogr.* **41**(11), 2080 (2011)

[28] A.Y. Shcherbina, M.A. Sundermeyer, E. Kunze, E. D'Asaro, G. Badin, D. Birch, A.M.E.G. Brunner-Suzuki, J. Callies, B.T.K. Cervantes, M. Claret, B. Concannon, J. Early, R. Ferrari, L. Goodman, R.R. Harcourt, J.M. Klymak, C.M. Lee, M.P. Long, M.D. Levine, R.C. Lien, A. Mahadevan, J.C. McWilliams, M.J. Molemaker, S. Mukherjee, J.D. Nash, T. Özgökmen, S.D. Pierce, S. Ramachandran, R.M. Samelson, T.B. Sanford, R.K. Shearman, E.D. Skillingstad, K.S. Smith, A. Tandon, J.R. Taylor, E.A. Terray, L.N. Thomas, J.R. Ledwell, *BAMS* **96**, 1257 (2015)

[29] D. Mukabi, G. Badin, N. Serra, *J. Phys. Oceanogr.* **46**(5), 1509 (2016)

[30] G. Badin, *Phys. Fluids* **26**(9), 096603 (2014)

[31] R. Blender, G. Badin, *J. Phys. A: Math. Theor.* **48**, 105501 (2015)

[32] P. Constantin, A. Majda, E. Tabak, *Nonlinearity* **7**, 1495 (1994)

[33] P. Constantin, A. Majda, E. Tabak, *Phys. Fluids* **6**(1), 9 (1994)

[34] A. Majda, E. Tabak, *Physica D* **98**(2-4), 515 (1996)

[35] K. Ohkitani, M. Yamada, *Phys. Fluids* **9**(4), 876 (1997)

[36] D. Córdoba, *Annals of Mathematics* **148**, 1135 (1998)

[37] P. Constantin, Q. Nie, N. Schorghofer, *Phys. Lett. A* **241**(3), 168 (1998)

[38] P. Constantin, J. Wu, *SIAM J. Math. Anal.* **30**(5), 937 (1999)

[39] D. Córdoba, C. Fefferman, *J. Am. Math. Soc.* **15**(3), 665 (2002)

[40] D. Córdoba, C. Fefferman, *Comm. Pure Appl. Math.* **55**(2), 255 (2002)

[41] A. Córdoba, D. Córdoba, *Comm. Math. Phys.* **249**(3), 511 (2004)

[42] J. Rodrigo, C. Fefferman, *Proc. Natl. Acad. Sci.* **101**(9), 2684 (2004)

[43] D. Córdoba, M. Fontelos, A. Mancho, J. Rodrigo, *Proc. Natl. Acad. Sci.* **102**(17), 5949 (2005)

[44] J. Rodrigo, *Comm. Pure Appl. Math.* **58**(6), 821 (2005)

[45] J. Wu, *Nonlinear Anal.* **62**(4), 579 (2005)

[46] J. Deng, T. Hou, R. Li, X. Yu, *Methods Appl. Anal.* **13**, 157 (2006)

[47] H. Dong, D. Li, *Proc. Am. Math. Soc.* **136**(7), 2555 (2008)

[48] N. Ju, *J. Diff. Eq.* **226**(1), 54 (2006)

[49] D. Li, *Nonlinearity* **22**(7), 1639 (2009)

[50] F. Marchand, *Comm. Math. Phys.* **277**(1), 45 (2008)

[51] F. Marchand, *Physica D* **237**(10), 1346 (2008)

[52] R. Scott, *J. Fluid Mech.* **687**, 492 (2011)

[53] P. Constantin, M.C. Lai, R. Sharma, Y.H. Tseng, J. Wu, *J. Sci. Comp.* **50**(1), 1 (2012)

[54] K. Ohkitani, *Phys. Fluids* **24**(9), 095101 (2012)

[55] R. Scott, D. Dritschel, *Phys. Rev. Lett.* **112**(14), 144505 (2014)

[56] R. Scott, D. Dritschel, *J. Fluid Mech.* **863**, R2 (2019)

- [57] J. Sukhatme, L.M. Smith, *Phys. Fluids* **21**(5), 056603 (2009)
- [58] L. Onsager, *Nuovo Cim.* **6**(2), 279 (1949)
- [59] G. Joyce, D. Montgomery, *J. Plasma Phys.* **10**(1), 107 (1973)
- [60] T.S. Lundgren, Y.B. Pointin, *J. Stat. Phys.* **17**(5), 323 (1977)
- [61] E. Caglioti, P.L. Lions, C. Marchioro, M. Pulvirenti, *Comm. Math. Phys.* **143**(3), 501 (1992)
- [62] E. Caglioti, P.L. Lions, C. Marchioro, M. Pulvirenti, *Comm. Math. Phys.* **174**(2), 229 (1995)
- [63] X. Carton, *J. Atmos. Sci.* **66**(4), 1051 (2009)
- [64] D. Dritschel, *Geophys. Astro. Fluid Dyn.* **105**(4-5), 368 (2011)
- [65] B. Harvey, M. Ambaum, *Geophys. Astro. Fluid Dyn.* **105**(4-5), 377 (2011)
- [66] B. Harvey, M. Ambaum, X. Carton, *J. Atmos. Sci.* **68**(5), 964 (2011)
- [67] E. Bembeneck, F. Poulin, M. Waite, *J. Phys. Oceanogr.* **45**(5), 1376 (2015)
- [68] X. Carton, D. Ciani, J. Verron, J. Reinaud, M. Sokolovskiy, *Geophys. Astro. Fluid Dyn.* **110**(1), 1 (2016)
- [69] G. Badin, F. Poulin, *Geophys. Astro. Fluid Dyn.* (2018). Doi:10.1080/03091929.2018.1453930
- [70] C. Lim, A. Majda, *Geophys. Astro. Fluid Dyn.* **94**(3-4), 177 (2001)
- [71] C. Taylor, S. Llewellyn Smith, *Chaos* **26**(11), 113117 (2016)
- [72] J.B. Weiss, A. Provenzale, J.C. McWilliams, *Phys. Fluids* **10**(8), 1929 (1998)
- [73] P.H. Chavanis, C. Sire, *Phys. Rev. E* **62**, 490 (2000)
- [74] O. Bühler, *Phys. Fluids* **14**(7), 2139 (2002)
- [75] P.H. Chavanis, *Eur. Phys. J. B* **70**(3), 413 (2009)
- [76] J. Esler, *Phys. Rev. Fluids* **2**(1), 014703 (2017)
- [77] J. Jimnez, *J. Fluid Mech.* **313**, 223 (1996)
- [78] I.A. Min, I. Mezic, A. Leonard, *Phys. Fluids* **8**(5), 1169 (1996)
- [79] J. Miller, *Phys. Rev. Lett.* **65**, 2137 (1990)
- [80] R. Robert, J. Sommeria, *Journal of Fluid Mechanics* **229**, 291 (1991)
- [81] R.S. Ellis, K. Haven, B. Turkington, *Nonlinearity* **15**(2), 239 (2002)
- [82] P.H. Chavanis, *Physica D* **200**(3), 257 (2005)
- [83] P.H. Chavanis, *Physica D* **237**(14), 1998 (2008)
- [84] P.H. Chavanis, A. Naso, B. Dubrulle, *Eur. Phys. J. B* **77**(2), 167 (2010)
- [85] F. Bouchet, M. Corvellec, *J. Stat. Mech.: Theory Exp.* **2010**(08), P08021 (2010)
- [86] A. Majda, X. Wang, *Nonlinear Dynamics and Statistical Theories for Basic Geophysical Flows* (Cambridge University Press, 2006)
- [87] T. Iwayama, T. Watanabe, *Phys. Rev. E* **82**, 036307 (2010)
- [88] H. Helmholtz, *J. Reine Angew. Math.* **55**, 25 (1858)
- [89] H. Aref, *J. Math. Phys.* **48**(6), 065401 (2007)
- [90] C. Marchioro, M. Pulvirenti, *Mathematical theory of incompressible nonviscous fluids*, vol. 96 (Springer Science & Business Media, 2012)
- [91] P. Newton, *The N-vortex problem: analytical techniques*, vol. 145 (Springer Science & Business Media, 2013)
- [92] D. Chapman, *J. Math. Phys.* **19**(9), 1988 (1978)
- [93] D.G. Dritschel, W. Qi, J.B. Marston, *J. Fluid Mech.* **783**, 1 (2015)
- [94] A.J. Majda, A.L. Bertozzi, *Vorticity and Incompressible Flow*. Cambridge Texts in Applied Mathematics (Cambridge University Press, 2001)
- [95] D.G. Dritschel, M. Lucia, A.C. Poje, *Phys. Rev. E* **91**, 063014 (2015)
- [96] F. Bouchet, A. Venaille, *Phys. Rep.* **515**(5), 227 (2012)
- [97] N. Fofonoff, *J. Mar. Res.* **13**, 254 (1954)
- [98] R.A. Pasmanter, *Phys. Fluids* **6**(3), 1236 (1994)
- [99] D. Gurarie, K.W. Chow, *Phys. Fluids* **16**(9), 3296 (2004)
- [100] F. Bouchet, J. Sommeria, *J. Fluid Mech.* **464**, 165 (2002)
- [101] M.T. Dibattista, A.J. Majda, B. Turkington, *Geophys. Astro. Fluid Dyn.* **89**, 235 (1998)
- [102] F. Bouchet, E. Simonnet, *Phys. Rev. Lett.* **102**, 094504 (2009)
- [103] A. Arakawa, *J. Comp. Phys.* **1**(1), 119 (1966)
- [104] T.Y. Hou, R. Li, *J. Comp. Phys.* **226**(1), 379 (2007)
- [105] F. Ragone, G. Badin, *J. Fluid Mech.* **792**, 740 (2016)
- [106] P. Tabeling, *Phys. Rep.* **362**(1), 1 (2002)
- [107] A.V. Pushkarev, W.J.T. Bos, *Phys. Fluids* **26**(11), 115102 (2014)
- [108] J. Beale, T. Kato, A. Majda, *Comm. Math. Phys.* **94**(1), 61 (1984)